Supporting Information

Significant Surface-enhanced Raman Scattering Effect of Ag Loaded Iron Hydroxide Enabled by Coordination Effect between Ag and Hydroxyl Group

Xiangyu Meng[‡a], Jian Yu[‡a], Jingjing Wu[a], Yuening Wang[a], Xiaoyu Song[a], Ziyan Xu[a], Anran Li[*a], Lin Qiu[*c] , Jie Lin[*b], and Xiaotian Wang [*a]

[a] School of Chemistry, and School of Engineering Medicine, Beijing Advanced Innovation Center for Big Data-Based Precision Medicine, Beihang University, Beijing 100191, China; Key Laboratory of Big Data-Based Precision Medicine (Beihang University), Ministry of Industry and Information Technology.

[b] Cixi Institute of Biomedical Engineering, Ningbo Institute of Materials Technology and Engineering, CAS, 1219 Zhongguan West Road, Ningbo 315201, P. R. China.

[c] School of Energy and Environmental Engineering, University of Science and Technology Beijing, Beijing 100083, China.

[‡] Co-first author. These two authors contributed equally to this manuscript.

[*]Corresponding authors. E-mail:

wangxt@buaa.edu.cn (Xiaotian Wang);

qiulin@ustb.edu.cn (Lin Qiu)

linjie@nimte.ac.cn (Jie Lin)

rananli@buaa.edu.cn (Anran Li)

Table S1. List of abbreviations.

Table S2. Raman spectral peak assignments of MB, CV, and 4ATP.

Figure S1. XRD of Ag NPs and Ag/ M hydroxide (M = Fe, Co, Ni) complex.

Figure S2. TEM image of commercial Ag NPs with the size of 5 nm.

Figure S3. XPS spectra of Fe^{3+}, Co^{2+} and Ni^{2+} in $Ag/Fe(OH)_3$, $Ag/Co(OH)_2$ and $Ag/Ni(OH)_2$, respectively.

Figure S4. Absorption spectra of $Fe(OH)_3$ and $Ag/Fe(OH)_3$.

Figure S5. TEM image of $Ag/Fe(OH)_3$ with different mass fraction of Ag.

Figure S6. The band gap of $Ag/Fe(OH)_3$ with different content of Ag based on the Kubelka-Munk formula.

Figure S7. (a) SERS intensity of 4-ATP with different concentration absorbed on 50% $Ag/Fe(OH)_3$. (b) SERS spectra of 4-ATP (10^{-4} M) absorbed on 50% $Ag/Fe(OH)_3$ and pure molecule (10^{-1} M) without substrate.

Table S1. List of abbreviations.

Number	Full forms	Abbreviation
1	Surface-enhanced Raman Scattering spectroscopy	SERS
2	P-aminoazobenzene	PAAB
3	Localized surface plasmon resonance	LSPR
3	Photo-induced charge transfer	PICT
4	Enhancement factor	EF
5	Electromagnetic enhancement mechanism	EM
6	Chemical enhancement mechanism	CM
7	Finite-difference time-domain	FDTD
8	X-ray powder diffraction	XRD
9	Transmission electron microscopy	TEM
10	X-ray pho-ton spectroscopy	XPS
11	Ultraviolet photoelectron spectroscopy	UPS
12	Selected area electron diffraction	SAED
13	Rhodamine 6G	R6G
14	Crystal violet	CV
15	4-aminophenylthiol	4-ATP
16	Conduction band	CB
17	Valence band	VB
18	Highest occupied molecular orbital	HOMO
19	Lowest unoccupied molecular orbital	LUMO

Table S2. Raman spectral peak assignments of MB, CV, and 4ATP.

	Raman shift (cm^{-1})	Assignments
R6G	1620	ν(C-C) ring
	1513	ν_{asym}(C-C)
	1430	ν_{asym}(C-N)
	1396	α(C-H)
	1307	α(C-H)
	1151	β(C-H)
	1181	ν(C-C)
	1035	β(C-H)
	677	γ(C-H)
CV	1615	ν(C-C) ring
	1588	ν(C-C) ring
	1532	ν(C-H) / $\delta(CH_3)$
	1447	$\gamma_{asym}(CH_3)$
	1396	ν(C-H)
	1180	ν(C-H) ring
	918	δ(C-C) ring
	818	ν(C-H) ring
	728	ν(C-N)
4-ATP	1590	ν(C-C) ring
	1575	ν(C-C) ring

1425	δ(CH) + ν(C-C)
1393	δ(C-H) + ν(C-C)
1142	δ(C-H)
1088	ν(C-S)

ν, stretching; α, in-plane deformation; β, in-plane bending; γ, out-of-plane bending; δ, skeletal deformation.

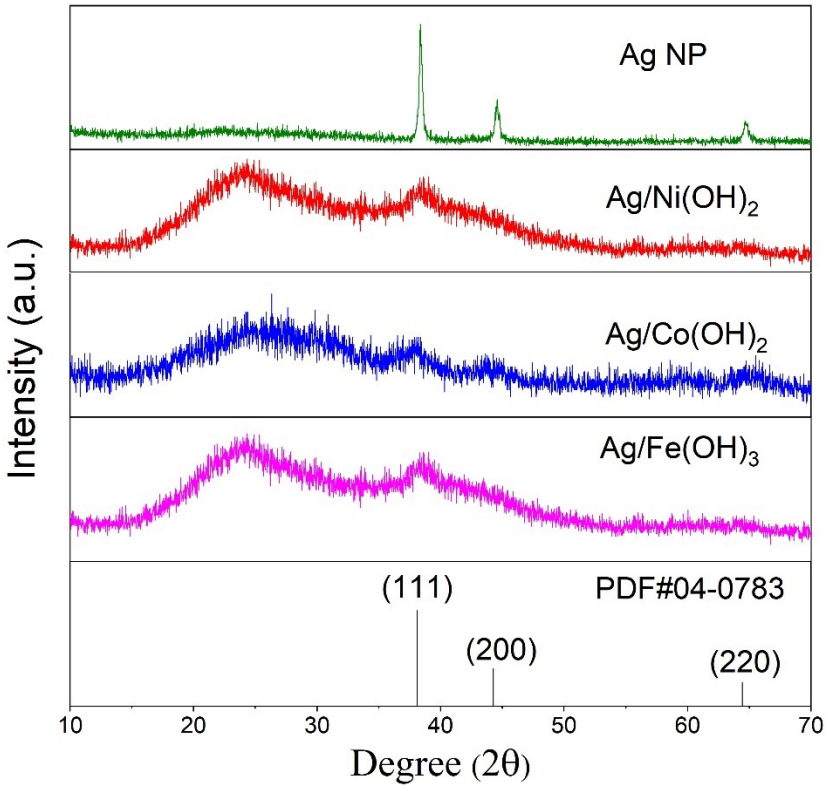

Figure S1. XRD of Ag NPs and Ag/M hydroxide (M = Fe, Co, Ni) complex.

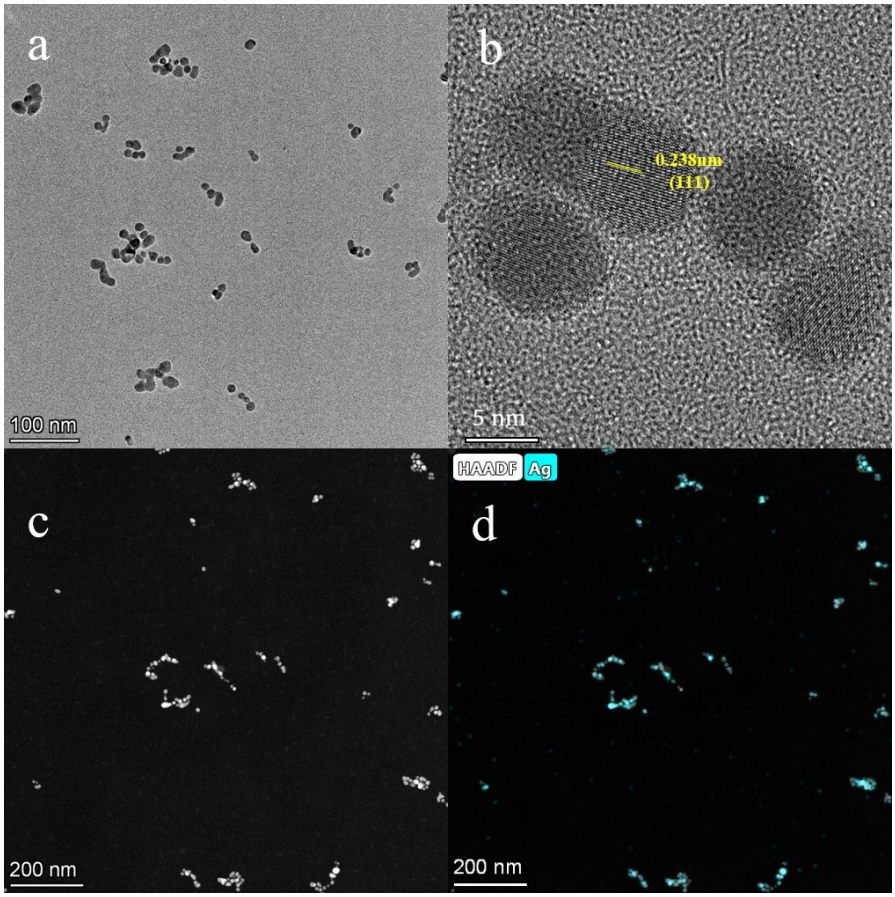

Figure S2. TEM image of commercial Ag NPs.

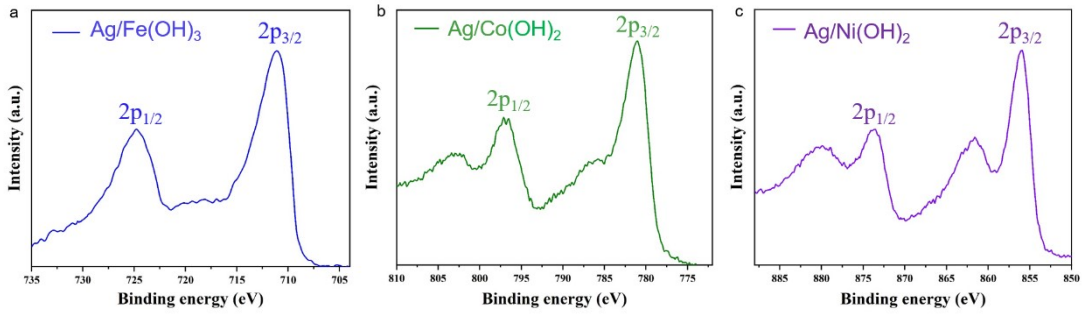

Figure S3. XPS spectra of Fe^{3+}, Co^{2+} and Ni^{2+} in $Ag/Fe(OH)_3$, $Ag/Co(OH)_2$ and $Ag/Ni(OH)_2$, respectively.

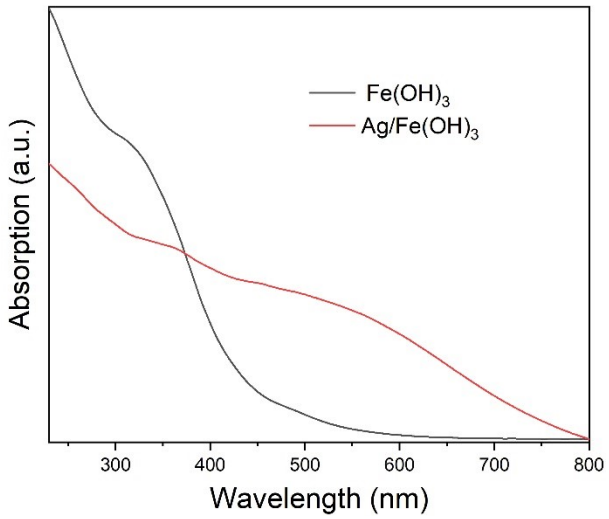

Figure S4. Absorption spectra of $Fe(OH)_3$ and $Ag/Fe(OH)_3$.

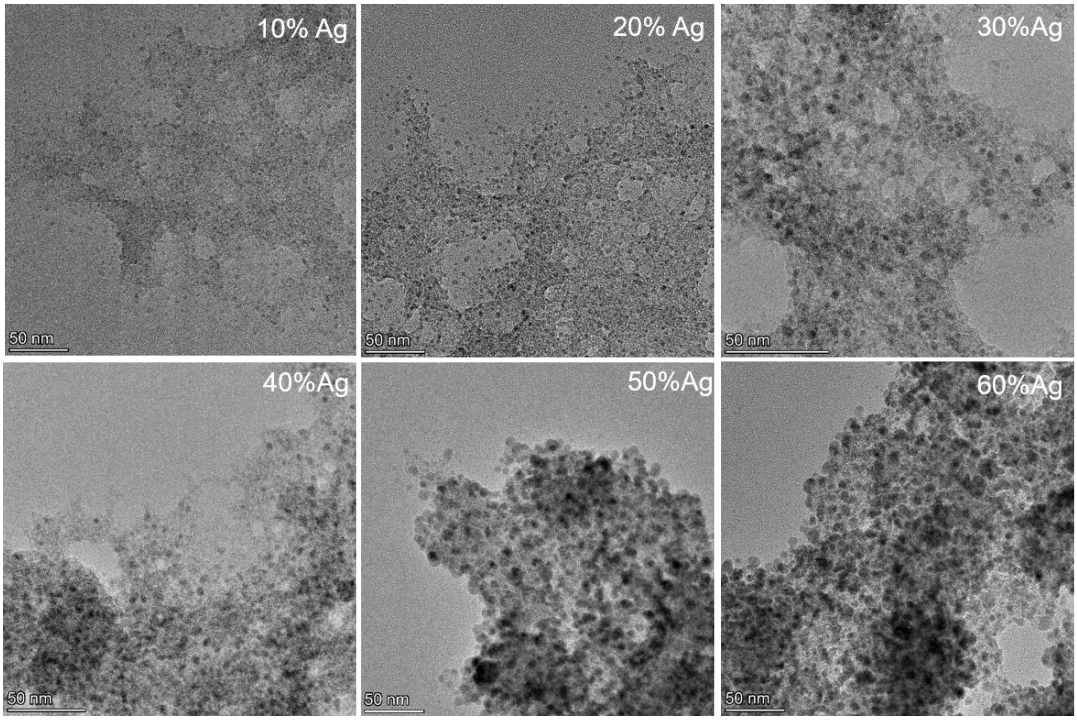

Figure S5. TEM image of Ag/$Fe(OH)_3$ with different mass fraction of Ag.

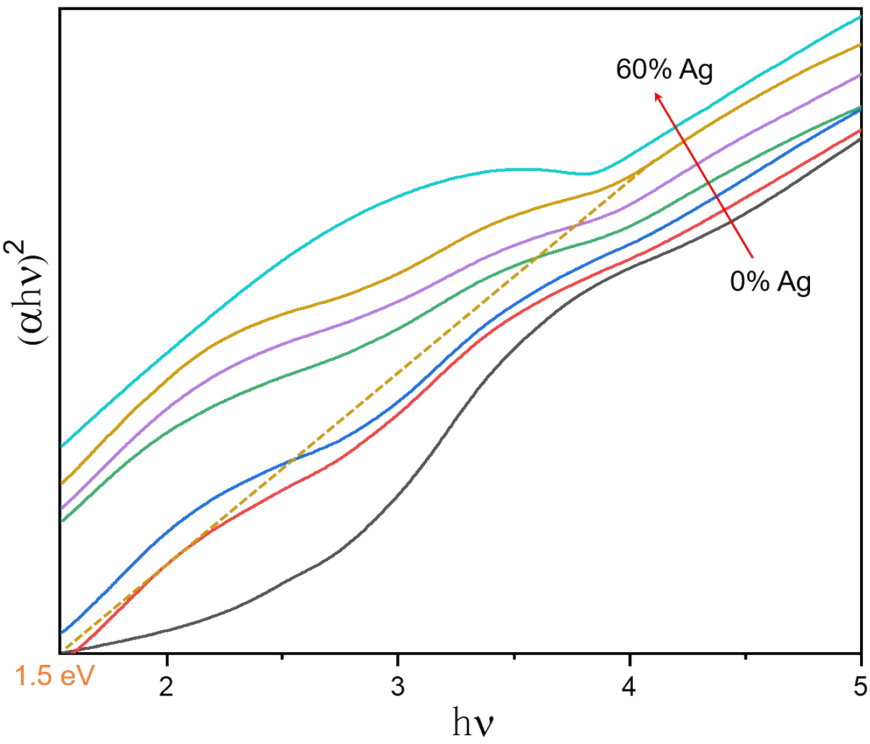

Figure S6. The band gap of Ag/$Fe(OH)_3$ with different content of Ag based on the Kubelka-Munk formula.

Calculation of Enhancement Factor

Figure S7 present the SERS intensity of 4-ATP with different concentration. The concentration of 10^{-4} M is selected to calculate the enhancement factor (EF) to avoid the error caused by supersaturated adsorption. EF for 50% Ag/$Fe(OH)_3$ is calculated by the following formula:

$$EF = \frac{I_{SERS}/N_{SERS}}{I_0/N_0} \qquad (1)$$

where I_{SERS} and I_0 is the intensity of vibration peaks of probe molecule absorbed on the substrate and without substrate (1590 cm^{-1} for 4-ATP). N_{SERS} and N_0 is the number of probe molecules on substrate and without the substrate, respectively.

In this experiment, 5uL of 4-ATP solution (0.1 M) was dropped onto the Si wafer (0.4×0.4 cm^{-2}). N_0 is estimated by:

$$N_0 = 5\ \mu L \times 0.1\ mol/L \times 6.02\times10^{23}\ mol^{-1} \times 1.87\ \mu m^2/0.16 cm^2$$

$$N_{SERS} = \sigma \times 1.87\ \mu m^2 \times 6.02\times10^{23}\ mol^{-1}$$

The laser area is calculated to be 1.87 μm^2 for the laser of 633 nm, and the area of Si wafer is 0.16 cm^2, N_0 is estimated to 3.51×10^{10}. σ is the density of probe molecule adsorbed onto substrate, which is estimated to ~0.5 nM cm^{-2}. Therefore, N_{SERS} is calculated to be 5.63×10^6 for 4-ATP and PAAB. I_{SERS}=11918 and I_0=60 for 4-ATP. Substituting these values into Eq. (1), EF are calculated to be 1.23×10^6 for 4-ATP.

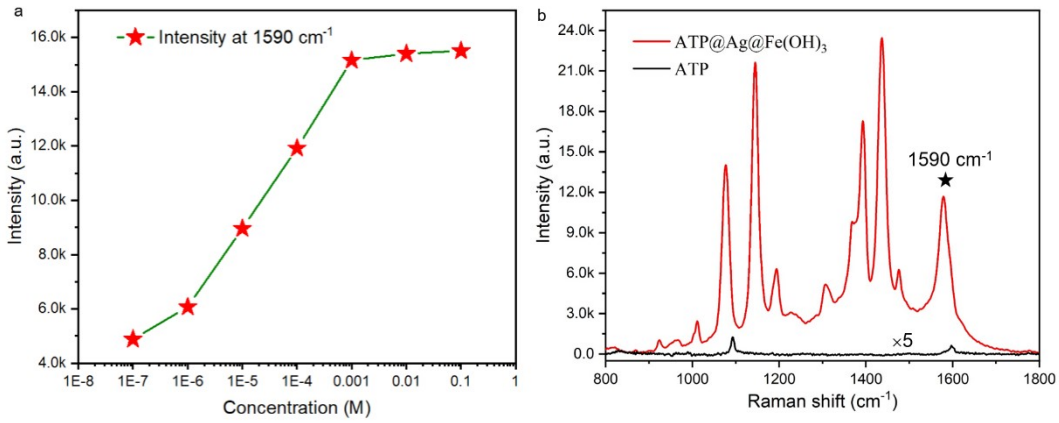

Figure S7. (a) SERS intensity of 4-ATP with different concentration absorbed on 50% $Ag/Fe(OH)_3$. (b) SERS spectra of 4-ATP (10^{-4} M) absorbed on 50% $Ag/Fe(OH)_3$ and pure molecule (10^{-1} M) without substrate.